journal

J. Am. Ceram. Soc., 93 [9] 2783–2787 (2010)
DOI: 10.1111/j.1551-2916.2010.03804.x

Antimony Tuned Rhombohedral-Orthorhombic Phase Transition and Enhanced Piezoelectric Properties in Sodium Potassium Niobate

Ruzhong Zuo,† Jian Fu, Danya Lv, and Yi Liu

Institute of Electro Ceramics & Devices, School of Materials Science and Engineering, Hefei University of Technology, Hefei 230009, China

It has been reported that the rhombohedral–orthorhombic low-temperature polymorphic phase transition in $(Na,K)NbO_3$ can be tuned close to room temperature by substituting Sb for Nb, such that enhanced piezoelectric properties are induced based on the theory of two-phase coexistence. A diagram of phase structures changing with Sb content and temperature has been generalized for $(Na,K)(Nb,Sb)O_3$ (NKNS) compositions. The thermal stability of piezoelectric properties of NKNS ceramics was evaluated considering the existence of successive phase transition above room temperature. The microstructure, dielectric, and ferroelectric properties of NKNS ceramics were discussed from a crystallographic point of view.

I. Introduction

THE $(Na_{0.5}K_{0.5})NbO_3$ has been considered to be a promising lead-free candidate material and has attracted much attention in recent years.[1–3] From low temperature to high temperature, it undergoes successive phase transitions: rhombohedral to orthorhombic (*r–o*) transition at ~ -123°C, orthorhombic to tetragonal (*o–t*) transition at ~ 200°C, and tetragonal to cubic (*t–c*) transition at ~ 410°C.[4] Like $BaTiO_3$, these phase transition temperatures can be adjusted by adding some dopants.[5] These additives might have different effects on the change of phase transition temperatures. The *o–t* polymorphic phase transition temperature (T_{o-t}) of $(Na_{0.5}K_{0.5})NbO_3$ appears to have attracted a great deal of attention in the last few years,[1,6–8] mainly because enhanced piezoelectric properties can be achieved based on the coexistence of orthorhombic and tetragonal ferroelectric phases when T_{o-t} is shifted near room temperature. By comparison, the *r–o* phase transition temperature (T_{r-o}) at low temperature has been almost neglected for this system.

Antimony has been widely used as a main modifier in $(Na,K)NbO_3$-based lead-free piezoelectric compositions. Our previous study[7] reported that excellent dielectric and piezoelectric properties could be obtained by fixing a relatively high amount of Sb in solid solutions of $(1-x)(Na,K)NbO_3$–$xLiTaO_3$ because it has a high electronegativity. However, a full study on the effect of Sb addition on the phase transition behavior of $(Na,K)NbO_3$ has rarely been carried out, particularly on the change of its low-temperature polymorphic phase transition. In this study, we showed that the T_{r-o} that is lower than room temperature can be tuned to above room temperature by forming a solid solution of $(Na_{0.52}K_{0.48})(Nb_{1-y}Sb_y)O_3$ ($NKNS_y$), where the content of Na is slightly more than that of K, considering a modified morphotropic phase boundary location in $(Na,K)NbO_3$.[9] Enhanced piezoelectric properties were discussed based on the coexistence of rhombohedral and orthorhombic phases.

II. Experimental Procedure

The $NKNS_y$ powder was synthesized via a conventional solid-state reaction method using high-purity carbonates and oxides: Na_2CO_3 (99.8%), K_2CO_3 (99.0%), Nb_2O_5 (99.5%), and Sb_2O_3 (99.9%) as raw materials. The as-calcined powders were mixed with 1 mol% CuO in order to reduce the sintering temperature and then underwent a ball-milling process for 24 h. Specimens were sintered in air in the temperature range of 1020°–1120°C for 3 h. For electrical measurements, silver paste was painted on major sides of the samples and fired at 550°C for 30 min. The samples were poled at 110°C in a silicone oil bath under a dc electric field of 2–4 kV/mm for 15 min.

The crystal structure of the ceramics was identified by a powder X-ray diffractometer (XRD, D/MAX2500VL/PC, Rigaku, Japan) using a Cu$K\alpha$1 radiation. The microstructure was observed using a scanning electron microscope (SEM, JEOL JSM-6490LV, Tokyo, Japan). The dielectric constant was measured as a function of temperature by an LCR meter (E4980A, Agilent, Santa Clara, CA) equipped with a temperature box filled with liquid nitrogen. Polarization versus electric field (*P–E*) hysteresis loops were measured using a ferroelectric measuring system (Precision LC, Radiant Technologies Inc., Albuquerque, NM). The piezoelectric constant d_{33} was measured by a Belincourt meter (YE2730A, Sinocera, Yangzhou, China). The mechanical quality factor Q_m was measured using a resonance–antiresonance method using an impedance analyzer (PV70A, Beijing Band ERA Co. Ltd., Beijing, China).

III. Results and Discussion

Figure 1 shows the XRD patterns at room temperature for $NKNS_y$ ceramics doped with 1 mol% CuO. It was found that most compositions exhibit a single perovskite structure, except for compositions with $y \geq 0.12$ where a small amount of secondary phase (Na_3SbO_3, ICDD: 44-0934) is detectable. The solubility of Sb in the NKN lattice is limited owing to the different crystal structures between $(Na,K)NbO_3$ (perovskite structure) and $(Na,K)SbO_3$ (pseudoilmenite structure). Moreover, it could be seen that the diffraction peaks shift to higher diffraction angles with increasing Sb content, indicating that there is a slight lattice shrinkage probably owing to a relatively small ionic radius of Sb^{5+} compared with that of Nb^{5+} (CN = 6, $R_{Sb} = 0.61$ Å, $R_{Nb} = 0.64$ Å).[10] It is worth noting that the addition of Sb has led to a change of crystal symmetry at room temperature for $NKNS_y$ samples. It was known that pure NKN has an orthorhombic symmetry at room temperature.[4] With the substitution of Sb for Nb ($y \geq 0.09$), the split diffraction peaks (002) and (200) merge gradually into a single one which should belong to either a rhombohedral or a cubic phase.

Furthermore, a Rietveld method via MAUD[11] was used to refine the structure parameters of $NKNS_y$ ceramics using the

D. Damjanovic—contributing editor

Manuscript No. 27251. Received December 15, 2009; approved March 20, 2010.

This work was financially supported by Key Project of Natural Science Research of Universities in Anhui Province (KJ2009A089), a project of Natural Science Foundation of Anhui Province (090414179), National Natural Science Foundation of China (50972035), and a Program for New Century Excellent Talents in University, State Education Ministry (NCET-08-0766).

†Author to whom correspondence should be addressed. e-mail: piezolab@hfut.edu.cn

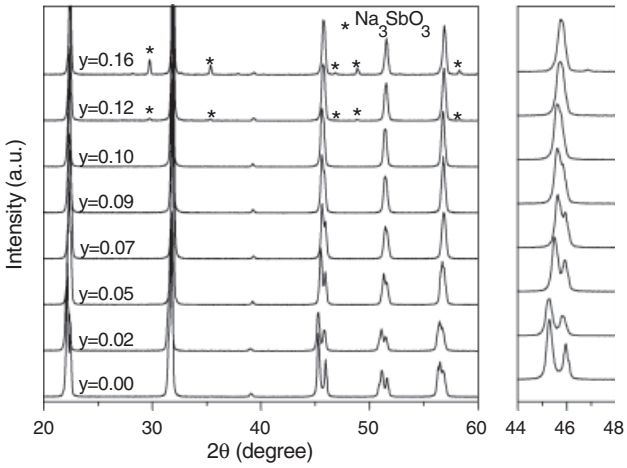

Fig. 1. X-ray diffractometer patterns of $NKNS_y$ ceramics sintered at 1100°C for 3 h; the magnified (200) diffraction peaks were shown on the right side.

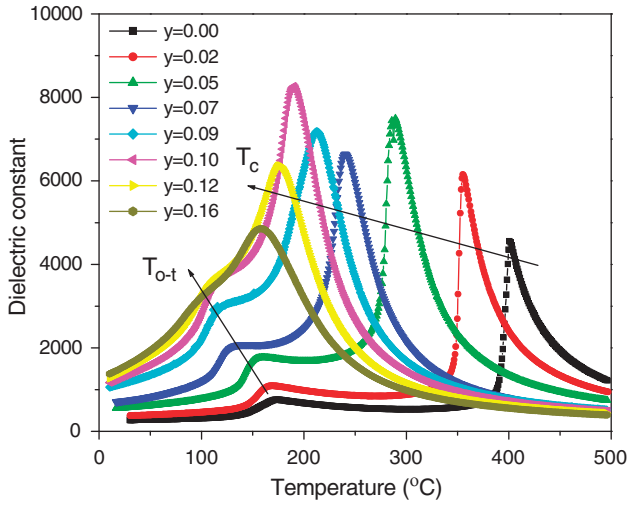

Fig. 2. Dielectric constant at 1 MHz in the temperature range of 20°–500°C for $NKNS_y$ ceramics as indicated.

XRD data shown in Fig. 1. The lattice parameters, primitive cell volumes V, space groups (SG) and reliability factor R_{wp}, and the goodness-of-fit indicator S are listed in Table I. The low S values suggest that the assigned structural models are reasonable. It was found that the structure can be well refined using an orthorhombic *Amm*2 model for $y \leq 0.07$ samples and a rhombohedral *R*3*m* symmetry model for $y \geq 0.09$ samples. The calculated lattice parameters and volumes first show slight shrinkage with increasing y up to 0.07; when $y \geq 0.09$, the volume undergoes a distinct increase owing to the phase structure transformation from orthorhombic *Amm*2 symmetry to rhombohedral *R*3*m* symmetry. Finally, it starts to decrease very slightly after $y = 0.12$, owing to the solubility limit.

The dielectric constant of unpoled $NKNS_y$ ceramics as a function of temperature was measured as shown in Figs. 2 and 3, considering that it appears anomalous at phase transition temperatures at a certain frequency. Three phase transition temperatures, T_{r-o}, T_{o-t}, and T_c (at *t*–*c* phase transition), can be distinguished clearly. Both T_{o-t} and T_c decrease with an increasing Sb content; however, the shift of T_c is faster than that of T_{o-t}, as shown in Fig. 2. Both of them still lie above room temperature within the solubility limit of Sb in NKN lattice. By comparison, the change of T_{r-o} can be recognized from Fig. 3. A dielectric anomaly, which should correspond to the *r*–*o* phase transition, starts to appear between room temperature and −60°C as $y \geq 0.02$. It was known that T_{r-o} is about −123°C for the $y = 0$ sample such that its corresponding dielectric peak is invisible within the studied temperature range. With increasing y, T_{r-o} moves close to room temperature against the direction of the T_{o-t} shift. T_{r-o} is higher than room temperature for $y \geq 0.09$ samples, which further confirms that the crystal symmetry at room temperature for $y \geq 0.09$ samples is rhombohedral rather than cubic because a ferroelectric should not possess centrosymmetry.

According to the above results, the phase transition behaviors of $NKNS_y$ ceramics can be summarized in Fig. 4. It can be seen that T_{r-o} changes faster than T_c and T_{o-t}. When $y = 0.09$, the *r*–*o* phase transition has been moved near room temperature and T_{o-t} and T_c are 115° and 190°C, respectively. A two-phase coexistence zone composed of rhombohedral and orthorhombic ferroelectric phases can be thereby formed near room temperature for compositions near $y = 0.09$, which is similar to the *o*–*t* phase transition induced phase coexistence in compositions such as Li-doped $(Na,K)NbO_3$.[12–14] Because of the solubility limit, no further change can be observed clearly for T_{r-o} and T_{o-t} when y is above 0.12. A slight decrease of T_c was observed if one compares samples with $y = 0.16$ and $y = 0.12$, mainly because the dielectric peak is suppressed and broadened by secondary phases with a low dielectric constant, as seen from Fig. 2. Moreover, it was found in this study that the shrinkage of the unit cell volume due to the substitution of a larger B cation (Nb^{5+}) with a smaller B cation (Sb^{5+}), which should induce a positive physical pressure, favors the low-temperature phase. This phenomenon is opposite to previous results for $BaTiO_3$ and $SrTiO_3$ in which a negative physical pressure stabilizes the low-temperature phase.[15,16]

Various electrical properties of $NKNS_y$ ceramics are shown in Fig. 5. It can be seen that electrical properties exhibit an obvious compositional dependence. The dielectric and piezoelectric properties increase with an increasing Sb content. The piezoelectric constant d_{33} reaches the optimum value ($d_{33} = 230$ pC/N) at approximately $y = 0.09$ and then starts to decrease with the addition of more Sb. The maximum values of piezoelectric properties at $y = 0.09$ could be attributed mainly to the coexistence of rhombohedral and orthorhombic ferroelectric phases. Therefore, the shift of the *r*–*o* phase transition close to room temperature tuned by means of various additives could provide a new approach toward the composition design of NKN-based lead-free ceramics. By comparison, the dielectric constant $\varepsilon_{33}^T/\varepsilon_o$ increases nearly linearly with y and becomes almost constant at higher values of y. This could be partially ascribed to both the solubility limit and the higher electronegativity of Sb. The latter tends to enhance the covalency of the composition and the off-center displacement,[1,17,18] such that dielectric and ferroelectric properties can be improved. Moreover, the *r*–*o* phase transition

Table I. Rietveld Refinement Parameters of $(Na_{0.52}K_{0.48})(Nb_{1-y}Sb_y)O_3$ Perovskite Ceramics

y	0	0.02	0.05	0.07	0.09	0.10	0.12	0.16
$a' = c'$ (Å)	4.0011	4.0002	3.9862	3.9770	3.9747	3.9714	3.9659	3.9627
b' (Å)	3.9556	3.9482	3.9466	3.9453	3.9747	3.9714	3.9659	3.9627
SG	*Amm*2	*Amm*2	*Amm*2	*Amm*2	*R*3*m*	*R*3*m*	*R*3*m*	*R*3*m*
V (Å^3)	63.32	63.18	62.71	62.40	62.79	62.64	62.38	62.23
R_{wp}	7.26	8.71	7.71	7.25	7.01	7.62	7.36	7.18
S	1.44	1.31	1.27	1.34	1.39	1.24	1.32	1.26

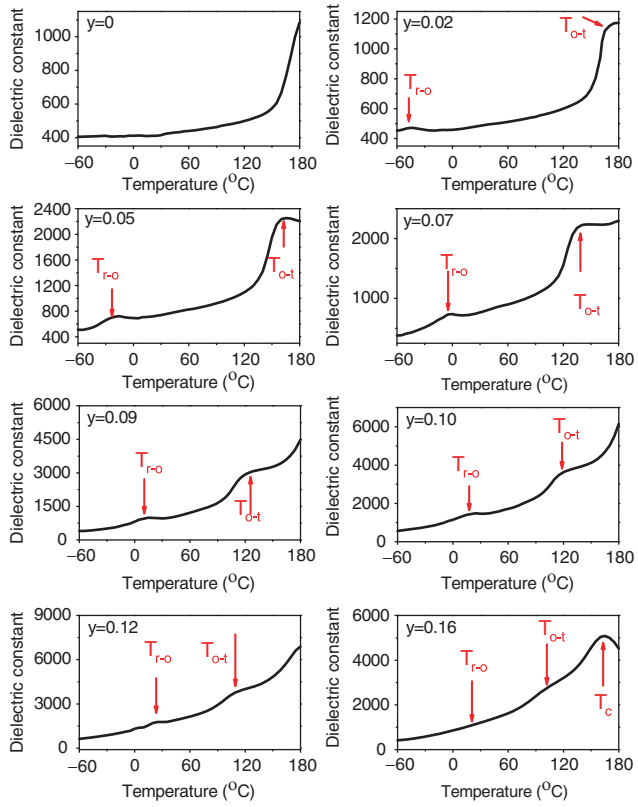

Fig. 3. Dielectric constant at 1 MHz in the temperature range of −60° to 180°C for $NKNS_y$ ceramics as indicated.

becomes more diffuse and broadened with an increasing Sb content (see Fig. 3), which could increase the dielectric constant as well. It is a pity that a rapid downshift of T_c occurs with increasing y (Fig. 2), which is undesirable for applications; however, the sample with $y = 0.09$ still possesses a T_c of >200°C.

In addition, the mechanical quality factor Q_m was found to decrease monotonously with the substitution of Sb, which indicates that Sb tends to make NKN ceramics electrically soft. The $y = 0$ samples have a relatively high Q_m value ($\sim$1450), owing to the addition of 1 mol% CuO as a sintering aid. It was known that CuO is an acceptor dopant and can make NKN ceramics electrically hard.[19,20] The softening effect of Sb addition can be attributed to both the formation of a two-phase coexistence zone caused by the shift of r–o phase transition ($Q_m = 102$ for the $y = 0.09$ sample), and enhanced dielectric and ferroelectric

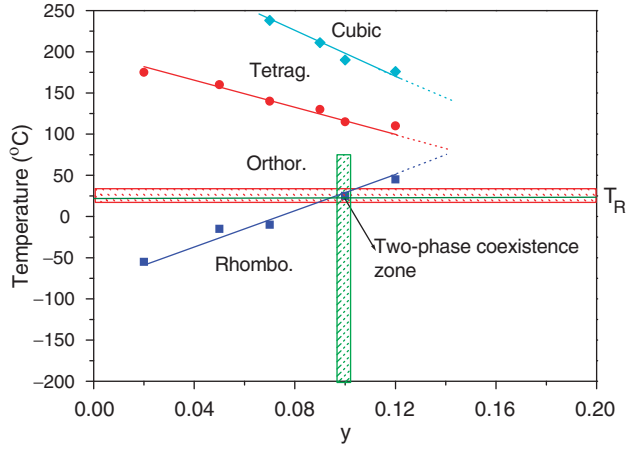

Fig. 4. Phase transition temperatures changing as a function of the Sb content y for $NKNS_y$ ceramics.

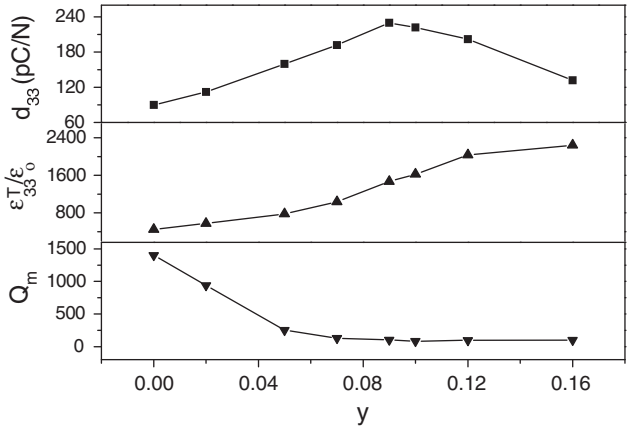

Fig. 5. Dielectric and piezoelectric properties of poled $NKNS_y$ ceramics sintered at optimum temperatures as a function of the Sb content y.

properties as discussed above. This influence can be clearly seen from P–E hysteresis loops of $NKNS_y$ ceramics, as shown in Fig. 6. The samples with low Sb content exhibit a typical double hysteresis-like loops, indicating that an evident hardening effect is generated. This can be explained using either a defect dipole theory or a space charge theory.[21,22] The former states that the defect dipoles could be formed between Cu'_{Nb}″ and $V_o^{\bullet\bullet}$ along the polarization direction, producing an inner bias field E_i to stabilize the polarization and thus increasing the Q_m value. The latter seems to correlate with the grain size. The space charges, i.e. charged defects such as Cu'_{Nb}″ and $V_o^{\bullet\bullet}$, move gradually toward the grain boundaries. The agglomerated space charges generate an E_i in the same direction of spontaneous polarization. However, this mechanism needs a long-range diffusion of space charges. Therefore, less E_i could be found in samples with a larger grain size because the formation of E_i needs the migration of space charges across bigger domains, as domain size was believed to increase with grain size.[23] However, the substitution of Sb leads to a clear reduction in grain size as shown in Fig. 7. The samples with a smaller grain size do not show a more evident hardening behavior, indicating that the space charge theory does not match well with the effect of Sb addition on the Q_m value in this case. As the Sb content y is ≥ 0.05, the hysteresis loops become normal and slim. More numbers of spontaneous polarization (P_s) vectors existing in samples with two-phase coexistence make the switching of polarization easier along the external electric field. The possible reason can be attributed to the fact that in a two-phase coexisted system, there is an increased number of directions along which P_s can be oriented. Free energies of the two phases coexisted are similar such that P_s can be switched easily among these different directions. The enhanced dielectric and ferroelectric properties due to the addition of Sb with a higher electronegativity also indicate a tendency to be electrically soft.

It can be noted that the sample with $y = 0.09$ not only has a r–o phase coexistence, but also has an additional o–t phase transition between room temperature and T_c. It should be interesting to explore its temperature dependence of piezoelectric properties induced by successive phase transformations upon heating. The thermal stability of piezoelectric properties was evaluated by measuring d_{33} values at room temperature after annealing poled samples at varying chosen annealing temperatures for 5 min. These values were normalized by dividing them by initial values of d_{33}. Normalized d_{33} values as a function of temperature are shown in Fig. 8. It is worth noting that d_{33} values decrease only slightly across the r–o phase boundary in the orthorhombic phase zone, whereas they decrease sharply across the o–t phase boundary in the tetragonal phase zone. That is to say, d_{33} values vary drastically with increasing temperature above T_{o-t} but change slightly between T_{r-o} and T_{o-t}. This indicates that the o–t phase boundary exhibits more temperature sensitivity than

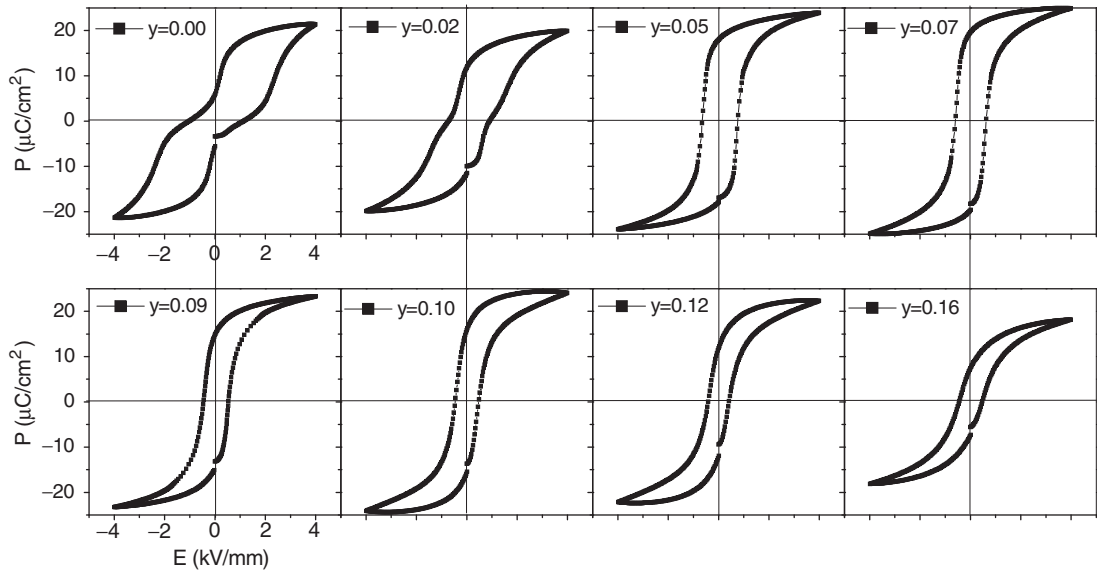

Fig. 6. Polarization versus electric field hysteresis loops of $NKNS_y$ ceramics sintered at optimum temperatures.

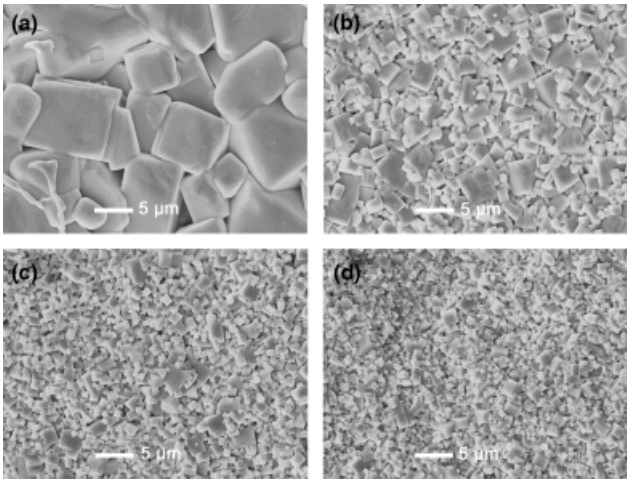

Fig. 7. Scanning electron microscope images of $NKNS_y$ ceramics sintered at 1100 °C for 3 h: (a) $y = 0$, (b) $y = 0.05$, (c) $y = 0.09$, and (d) $y = 0.16$.

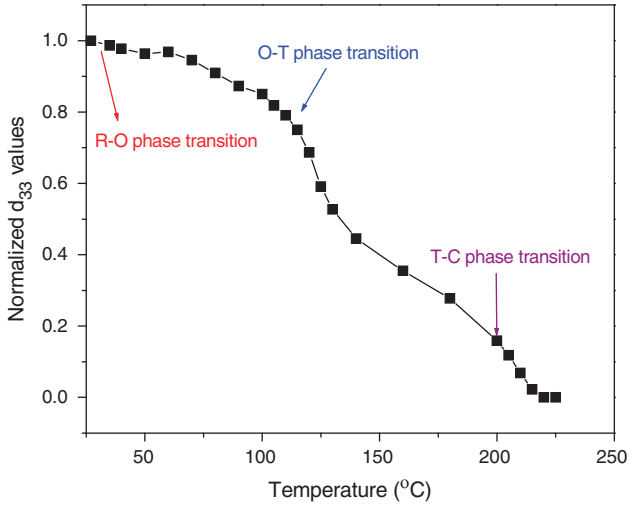

Fig. 8. Temperature dependence of piezoelectric constant d_{33} of poled samples with $y = 0.09$.

the *r–o* phase boundary. A similar phenomenon was observed in $BaTiO_3$-based materials.[24] In addition, it can be seen that the peak of d_{33} values at the location of T_{o-t} has been smeared owing to the partial overlap of *r–o* and *o–t* phase transition zone. These behaviors appear different from those in Li-doped NKN ceramics with the O and T phase coexistence.[25] The shift of the *r–o* phase transition closer to room temperature tuned by some additives provides a new approach toward the design of new lead-free ceramics based on NKN compositions.

IV. Conclusions

In this study, it was demonstrated that the incorporation of Sb into the NKN lattice favors its low-temperature crystal structure such that the *r–o* phase transition temperature can be tuned near room temperature at approximately $y = 0.09$, where the material shows optimum piezoelectric properties of $d_{33} = 230$ pC/N, $\varepsilon_{33}^T/\varepsilon_o = 1470$, and $Q_m = 102$. The existence of successive polymorphic phase transitions above room temperature makes the samples exhibit different thermal stability characteristics from previously reported NKN-based lead-free ceramics.

References

[1]Y. Saito, H. Takao, T. Tani, T. Nonoyama, K. Takatori, T. Homma, T. Nagaya, and M. Nakamura, "Lead-Free Piezoceramics," *Nature*, **432**, 84–7 (2004).

[2]T. R. Shrout and S. J. Zhang, "Lead-Free Piezoelectric Ceramics: Alternatives for PZT," *J. Electroceram.*, **19**, 111–24 (2007).

[3]J. Rodel, W. Jo, K. T. P. Seifert, E. M. Anton, T. Granzow, and D. Damjanovic, "Perspective on the Development of Lead-Free Piezoceramics," *J. Am. Ceram. Soc.*, **92**, 1153–77 (2009).

[4]H. J. Trodahl, N. Klein, D. Damjanovic, N. Setter, B. Ludbrook, D. Rytz, and M. Kuball, "Raman Spectroscopy of $(K,Na)NbO_3$ and $(K,Na)_{1-x}Li_xNbO_3$," *Appl. Phys. Lett.*, **93**, 262901 (2008).

[5]B. Jaffe, W. R. Cook, and H. Jaffe, *Piezoelectric Ceramics*. Academic Press, New York, 1971.

[6]E. K. Akdogan, K. Kerman, M. Abazari, and A. Safari, "Origin of High Piezoelectric Activity in Ferroelectric $(K_{0.44}Na_{0.52}Li_{0.04})(Nb_{0.84}Ta_{0.1}Sb_{0.06})O_3$ Ceramics," *Appl. Phys. Lett.*, **92**, 112908 (2008).

[7]R. Z. Zuo, J. Fu, and D. Y. Lv, "Phase Transformation and Tunable Piezoelectric Properties of Lead-Free $(Na_{0.52}K_{0.48-x}Li_x)(Nb_{1-x-y}Sb_yTa_x)O_3$ System," *J. Am. Ceram. Soc.*, **92**, 283–5 (2009).

[8]J. L. Zhang, X. J. Zong, L. Wu, Y. Gao, P. Zheng, and S. F. Shao, "Polymorphic Phase Transition and Excellent Piezoelectric Performance of $(K_{0.55}Na_{0.45})_{0.965}Li_{0.035}Nb_{0.80}Ta_{0.20}O_3$ Lead-Free Ceramics," *Appl. Phys. Lett.*, **95**, 022909 (2009).

[9]Y. J. Dai, X. W. Zhang, and K. P. Chen, "Morphotropic Phase Boundary and Electrical Properties of $K_{1-x}Na_xNbO_3$ Lead-Free Ceramics," *Appl. Phys. Lett.*, **94**, 042905 (2009).

[10]R. D. Shannon, "Revised Effective Ionic Radii and Systematic Studies of Interatomic Distances in Halides and Chalcogenides," *Acta Cryst. A*, **32**, 751–67 (1976).
[11]P. Sahu, S. K. Pradhan, and M. De, "X-Ray Diffraction Studies of the Decomposition and Microstructural Characterization of Cold-Work Powders of Cu-15Ni–Sn Alloys by Rietveld Analysis," *J. Alloys Compd.*, **377**, 103–16 (2004).
[12]Y. P. Guo, K. Kakimoto, and H. Ohsato, "Phase Transitional Behavior and Piezoelectric Properties of $(Na_{0.5}K_{0.5})NbO_3$–$LiNbO_3$ Ceramics," *Appl. Phys. Lett.*, **85**, 4121–3 (2004).
[13]E. Hollenstein, M. Davis, D. Damjanovic, and N. Setter, "Piezoelectric Properties of Li- and Ta-Modified $(K_{0.5}Na_{0.5})NbO_3$ Ceramics," *Appl. Phys. Lett.*, **87**, 182905 (2005).
[14]B. Q. Ming, J. F. Wang, P. Qi, and G. Z. Zang, "Piezoelectric Properties of (Li, Sb, Ta) Modified (Na, K)NbO_3 Lead-Free Ceramics," *J. Appl. Phys.*, **101**, 054103 (2007).
[15]W. Zhong, D. Vanderbilt, and K. M. Rabe, "First-Principles Theory of Ferroelectric Phase Transitions for Perovskites: The Case of $BaTiO_3$," *Phys. Rev. B*, **52**, 6301–12 (1995).
[16]R. Wordenweber, E. Hollmann, R. Kutzner, and J. Schubert, "Induced Ferroelectricity in Strained Epitaxial $SrTiO_3$ Films on Various Substrates," *J. Appl. Phys.*, **102**, 044119 (2007).
[17]R. E. Cohen, "Origin of Ferroelectricity in Perovskite Oxides," *Nature*, **358**, 136–8 (1992).
[18]R. E. Cohen, "Relaxors Go Critical," *Nature*, **441**, 941–2 (2006).
[19]M. Matsubara, T. Yamaguchi, W. Sakamoto, K. Kikuta, T. Yogo, and S. Hirano, "Processing and Piezoelectric Properties of Lead-Free (K, Na)(Nb, Ta)O_3 Ceramics," *J. Am. Ceram. Soc.*, **88**, 1190–6 (2005).
[20]D. M. Lin, K. W. Kwok, and H. L. W. Chan, "Double Hysteresis Loop in Cu-Doped $K_{0.5}Na_{0.5}NbO_3$ Lead-Free Piezoelectric Ceramics," *Appl. Phys. Lett.*, **90**, 232903 (2007).
[21]P. V. Lambeck and G. H. Jonker, "Ferroelectric Domain Stability in $BaTiO_3$ by Bulk Ordering of Defects," *Ferroelectrics*, **22**, 729–31 (1978).
[22]K. Okazaki and H. Maiwa, "Space Charge Effects on Ferroelectric Ceramic Particle Surfaces," *Jpn. J. Appl. Phys.*, **31**, 3113–6 (1992).
[23]W. Cao and C. A. Randall, "Grain Size and Domain Size Relations in Bulk Ceramic Ferroelectric Materials," *J. Phys. Chem. Solids*, **57**, 1499–505 (1996).
[24]P. Zheng, J. L. Zhang, S. F. Shao, Y. Q. Tan, and C. L. Wang, "Piezoelectric Properties and Stabilities of CuO-Modified Ba(Ti,Zr)O_3 Ceramics," *Appl. Phys. Lett.*, **94**, 032902 (2009).
[25]K. Higashide, K. Kakimoto, and H. Ohsato, "Temperature Dependence on the Piezoelectric Property of $(1-x)(Na_{0.5}K_{0.5})NbO_3$–$xLiNbO_3$ Ceramics," *J. Eur. Ceram. Soc.*, **27**, 4107–10 (2007). □